

## Interaction between physical and chemical weathering of argillaceous rocks and the effects on the occurrence of acid mine drainage (AMD)

Matsumoto, Shinji

Department of Earth Resources Engineering, Faculty of Engineering, Kyushu University

Shimada, Hideki

Department of Earth Resources Engineering, Faculty of Engineering, Kyushu University :  
Professor

Sasaoka, Takashi

Department of Earth Resources Engineering, Faculty of Engineering, Kyushu University :  
Associate Professor

<https://hdl.handle.net/2324/4355477>

---

出版情報 : Geosciences Journal. 21 (3), pp.397-406, 2017-05-09. Springer Nature  
バージョン :  
権利関係 :

1 **Interaction between physical and chemical weathering of argillaceous rocks and**  
2 **the effects on the occurrence of acid mine drainage (AMD)**

3

4 Shinji Matsumoto<sup>1\*</sup>, Hideki Shimada<sup>1</sup>, Takashi Sasaoka<sup>1</sup>

5 1. Department of Earth Resources Engineering, Kyushu University, Fukuoka, Nishiku,  
6 Motooka 744, Japan

7

8 Shinji Matsumoto<sup>1\*</sup>, e-mail: shinji12@kyudai.jp

9 Hideki Shimada<sup>1</sup>, e-mail: shimada@mine.kyushu-u.ac.jp

10 Takashi Sasaoka<sup>1</sup>, e-mail: sasaoka@mine.kyushu-u.ac.jp

11

12 Short running title:

13 **Interaction between physical and chemical weathering of argillaceous rocks**

14

15

16

---

\* Corresponding author: shinji12@kyudai.jp  
Tel: +81928023334; Fax: +81928023368

17 **Abstract:** The disintegration of rocks by weathering plays an important role in the  
18 occurrence of Acid Mine Drainage (AMD), which is the environmental problem  
19 caused by the exposure of sulfide minerals to water and oxygen. The weathering  
20 of rocks is, generally, classified into physical or chemical weathering. However,  
21 there are few studies that focus on the complex interaction between physical and  
22 chemical weathering of rocks and on the effects of the interaction on the  
23 occurrence of AMD. This paper elucidates the complex interrelation between  
24 physical and chemical weathering of rocks as well as the progress of AMD  
25 through leaching test and weathering test with argillaceous rocks taken in  
26 open-cast coal mine in Indonesia in addition to sample analysis before and after  
27 the wetting and drying cycle: the rock samples were exposed to oxygen and water  
28 during the cycle. The results indicated that the argillaceous rocks which consist of  
29 sulfide and/or sulfate caused chemical weathering with micro-cracks on the  
30 surface of rocks through the dissolution of soluble iron and sulfur during the  
31 occurrence of AMD. Additionally, physical weathering of rocks due to clay  
32 minerals was accelerated by chemical weathering with the development of cracks  
33 with the occurrence of AMD in the argillaceous rocks containing kaolinite and  
34 pyrite. Although weathering of rocks also accelerated AMD, it was concluded that

35 the sulfur content, the form of sulfur and iron in rocks, and the supply of oxygen  
36 significantly contributed to the occurrence of AMD.

37

38 **Keywords:** Acid Mine Drainage (AMD), physical weathering, chemical  
39 weathering, argillaceous rocks

40

41

42

43

44

45

46

47

48

49

50

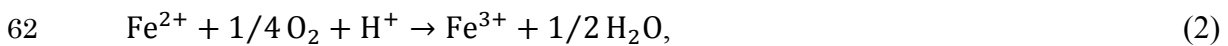
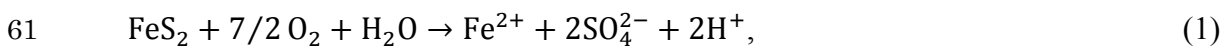
51

52

53 **1. INTRODUCTION**

54 Acid Mine Drainage (AMD), which is the environmental problem caused by the  
55 exposure of sulfide minerals to water and oxygen, has a negative impact on the  
56 ecosystem in the surrounding area owing to low-pH and heavy metals dissolved with  
57 the decrease of pH (Jennings et al., 2008). It is mainly caused by the oxidation of pyrite,  
58 and the main oxidants are O<sub>2</sub> and Fe<sup>3+</sup> as shown in Eq. (1) and Eq. (3). Firstly, Fe<sup>2+</sup> is  
59 dissolved from pyrite (Eq. (1)), and Fe<sup>2+</sup> is oxidized to Fe<sup>3+</sup> by O<sub>2</sub> (Eq. (2)).

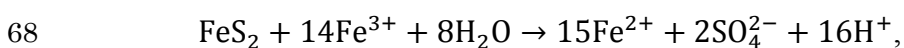
60



63

64 With the reaction progress as presented above, the pH decreases. The oxidation of pyrite  
65 is, moreover, accelerated by Fe<sup>3+</sup> which is strong oxidant (Eq. (3)). Depending on pH,  
66 Fe<sup>3+</sup> precipitates as Fe(OH)<sub>3</sub> (Eq. (4)).

67



69 (3)



71

72 To carry out effective measures against AMD, it is necessary to elucidate the  
73 mechanism and the cause of AMD. The weathering of rocks is one of the key factors for  
74 understanding the progress of AMD in nature since the weathering of rocks easily  
75 occurs under acid conditions, and it causes the release of most of the elements (Jennings  
76 et al., 2008; Dold et al., 2013). The weathering of rocks is classified into physical or  
77 chemical weathering by the types of the cause of the weathering such as rain, snow,  
78 wind and temperature, resulting in a complex mechanism of the progress of the  
79 weathering of rocks (Lobb and Femmer, 2007; Moon and Jayawardane, 2004). Since  
80 the weathering of rocks can affect the occurrence of AMD through the increase of  
81 reactive area of rocks with the disintegration, the progress of AMD has to be  
82 investigated in terms of physical and chemical weathering of rocks. However, there are  
83 few studies that focus on the complex interaction between physical and chemical  
84 weathering of rocks and the effects of the interaction on the occurrence of AMD.

85 In this study, leaching test and weathering test were conducted with argillaceous rock  
86 which is a sedimentary rock formed by clay and taken in open-cast coal mine in  
87 Indonesia in addition to sample analysis before and after the wetting and drying cycle:  
88 the rock samples were exposed to oxygen and water during the cycle. On the basis of

89 the results, we examined the interaction between physical and chemical weathering of  
90 rocks as well as the effect of the interaction on AMD.

91

## 92 2. MATERIALS AND METHODS

### 93 2.1. Rock Samples and Analytical Methods

94 Rock samples were collected in pit in the coal mine in Indonesia where the  
95 weathering of rocks and the occurrence of AMD have been reported owing to heavy  
96 rain and high temperature in the tropical climate. Four samples which were not exposed  
97 to the atmosphere were taken from the wall in pit, followed by sample analysis in a  
98 laboratory. All samples were categorized as argillaceous rock according to geological  
99 data in the mine. They were named as sample A, B, C, and D, respectively. These  
100 samples were dried at 50°C in a nitrogen atmosphere for 24 hours to supply for X-ray  
101 Diffraction (XRD) and X-ray Fluorescence (XRF) analysis. Major minerals in the  
102 samples were analyzed using the X-ray diffractometer (Rigaku, Ultima IV, Japan) under  
103 the following condition: radiation CuK $\alpha$ , operating voltage 40 kV, current 26 mA,  
104 divergence slid 1 deg, anti-scatter 1deg, receiving slit 0.3 mm, step scanning 0.050°,  
105 scan speed 2.000°/min, scan range 2.000-65.000°. In addition, quartz index (QI) was  
106 calculated based on the results of XRD analysis in order to compare the mineral content

107 of the samples. QI was calculated by dividing the maximum intensity ( $I_m$ ) of the target  
108 mineral in the sample by X-ray intensity of 100 wt% of standard quartz ( $I_p$ ) which was  
109 measured under the same conditions as follows (Okawara et al., 1996):

$$110 \quad \text{QI} = I_m / I_p \times 100$$

111 Whereas QI is affected by the effect of X-ray mass-absorption coefficient and the  
112 difference of reflected intensity at the bottom of minerals, it can be used to compare the  
113 mineral content relative to the same type of mineral in other samples (Okawara et al.,  
114 1996).

115

## 116 **2.2. Leaching Test**

117 Leaching test was performed with sample A, B, C and D so as to understand the acid  
118 generating potential of the samples. After sieving the samples into 1.5-2.0 mm, they  
119 were packed into a glass column (40.4 mm diameter × 58.9 mm height). 10 mm  
120 thickness of a supporting layer was installed by setting paper filter, 0.5-1.0 mm of glass  
121 beads, and sieves at the bottom of the column to support the samples. In order to unify  
122 the reactive area of the samples in each column, the porosity was calculated using the  
123 density of the samples and the volume of filling the samples and set at 60%. 100 ml of  
124 distilled water was poured into the column and the leachate was sampled from the



125 bottom of the column for the measurement of pH, followed by the drying process by  
126 using an artificial light for 24 hours. The weight of the samples after pouring distilled  
127 water was confirmed to decrease to the initial weight of the samples at the end of the  
128 drying process. After the wetting and drying cycle was repeated until 10 times, 14 days  
129 of the drying process was prepared without an artificial light. The step of 10 times of the  
130 wetting and drying cycle with 14 days of the drying process was, furthermore, repeated  
131 until 3 times. The total number of the supply of 100 ml of distilled water was 30 times  
132 in this study on the assumption of annual rainfall in the mine area in Indonesia. Thus,  
133 the wetting and drying cycle was attributed to the supply of distilled water and the heat  
134 of the artificial light in this experiment. Additionally, 20.6% of O<sub>2</sub> was measured with  
135 oxygen meter (Toray, LC-450F, Japan) at the top and the bottom of the column at the  
136 end of every drying process, indicating that same amount of oxygen was supplied to the  
137 samples in each column during the drying process. At the end of the leaching test, grain  
138 size analysis was, besides, conducted so that the progress of the weathering of rocks  
139 with the occurrence of AMD during the leaching test was examined.

140  
141  
142

### 143 2.3. Slaking Index (SI) Test to Understand Physical Weathering of Rocks

144 Slaking of rocks which is caused by the swelling pressure of clay minerals through  
145 the wetting and drying cycle is classified into physical weathering of rocks  
146 (Karathanasis et al., 2014). In this study, Slaking Index (SI) test was performed to  
147 understand the slaking behavior of the rock samples (Sadisun et al., 2003). Less than 2  
148 mm of the samples was removed by sieving and the weight of more than 2 mm of the  
149 samples was measured after the wetting and drying cycle in SI test. SI was calculated as  
150 the indicator of slaking using the change of the weight of the samples until 5 times.

151

### 152 2.4. Acid Extraction Test to Understand Chemical Weathering of Rocks

153 Acid extraction test was carried out by reference to the analysis conducted by Sasaki  
154 et al. (2002) to elucidate the form of sulfur and iron in the rock samples since the  
155 dissolution rate of elements depends on the form of minerals (Sasaki et al., 2002).  
156 Minerals can be extracted with acids at each stage of the extraction (Huerta-Diaz and  
157 Morse, 1990). 2.5 g of dried sample was dissolved with 20 ml of 1 mol/dm<sup>3</sup>  
158 hydrochloric acid (HCl), 60 ml of 46% hydrogen fluoride (HF), and 10 ml of conc.  
159 nitric acid (HNO<sub>3</sub>) in line with the method in the past research (Sasaki et al., 2002).  
160 Sasaki et al. (2002) mentioned that soluble minerals were extracted with HCl, and

161 silicate minerals were extracted with HF, and refractory minerals such as sulfide  
162 minerals were extracted with HNO<sub>3</sub>. In this study, the time of shaking of the mixture at  
163 HNO<sub>3</sub> step was changed from 2 hours in the past research to 6 hours in order to dissolve  
164 sulfide minerals completely. The proportion of each form of sulfur and iron composing  
165 pyrite was calculated based on the amount of extracted sulfur and iron (mg/g) from rock  
166 samples.

167

## 168 **2.5. Simple Dissolution Test and Scanning Electron Microscopy (SEM)**

### 169 **Observation**

170 Simple dissolution test was conducted by reference to the standard of the pH<sub>1:2</sub> test of  
171 AMIRA in addition to the acid extraction test so as to observe the chemical weathering  
172 of rocks: the ratio of solid to liquid was 1:2 (AMIRA, 2002). The size of samples was  
173 changed from -75 μm in the standard to 1.0 mm in order to clearly observe the change  
174 of surface conditions of the samples before and after the simple dissolution test using  
175 Scanning Electron Microscopy (SEM). The sample which underwent the wetting and  
176 drying cycle was used to compare the amount of extracted iron and sulfur with HCl in  
177 the acid extraction test and the amount of dissolved sulfur and iron in the leachate in the  
178 simple dissolution test. The leachate was supplied to Inductively Coupled

179 Plasma-Atomic Emission Spectrometry (ICP-AES) to measure the concentration of  
180 sulfur and iron soon after the simple dissolution test in order not to accelerate the  
181 reaction of the samples with oxygen and water. The results were calculated using the  
182 unit of mg/g to compare the results of the simple dissolution test and the acid extraction  
183 test. Besides, the samples after the simple dissolution test were dried by lyophilizer  
184 filled with nitrogen gas to prevent the oxidation of the samples before the observation  
185 using SEM. The progress of chemical weathering of rocks was investigated based on  
186 the change of surface conditions of the rock samples before and after the simple  
187 dissolution test.

188

### 189 3. RESULTS AND DISCUSSION

190 In order to clarify each experiment and the purpose, the experimental scheme is  
191 presented in Table 1.

192

193

194

**Table 1.**

195

196

197 **3.1. Acid Generating Potential of Rock Samples**

198 The XRD patterns of the rock samples are shown in Figure 1. The peaks of quartz  
199 and kaolinite were found in all samples. The peaks of pyrite were clearly observed in  
200 sample B and D, indicating that the content of pyrite was high in sample B and D. The  
201 peaks of albite were clearly seen in only sample A, B, and C, while it was not found in  
202 sample D. Additionally, only sample A contained siderite based on the result in Figure 1.  
203 Table 2 shows QI which was calculated using the intensity of each mineral in Figure 1,  
204 and Figure 2 shows the chemical component of the samples: others in sample B and D  
205 were mostly composed of water. Although QI of quartz was quite low in sample D,  
206 similar values of QI of kaolinite were obtained in all samples. Besides, QI of albite was  
207 slightly higher in sample C. The content of silica in each sample in Figure 2 was  
208 supported by QI of quartz in Table 2. Moreover, a large amount of iron and sulfur in  
209 sample B and D in Figure 2 was well correlated with the peaks of pyrite in the samples  
210 in Figure 1. Pyrite was not observed in sample A and C in Figure 1; however, the sulfur  
211 content was 0.83% and 0.03% in sample A and C, respectively. This suggested that  
212 sample A and C may contain small amount of sulfide causing AMD.

213

214

215

216

217

**Fig. 1.**

218

219

220

**Table 2.**

221

222

223

**Fig. 2.**

224

225

226 Figure 3 shows the change of pH in the leaching test. The change of pH can be

227 classified into two groups. The pH in sample B and D remained at pH 2.0-3.0, while

228 sample C showed a rapid increase in pH at the early step of leaching, followed by a

229 gradual increase at pH 7.0-8.0. Furthermore, sample A showed a gradual increase in pH

230 overall. As the content of pyrite was high in sample B and D, the pH in sample B and D

231 remained at low-pH with the dissolution of pyrite in the leaching test. On the other hand,

232 the pH gradually increased in sample A and C because of the low content of sulfur.

233 During the drying process in the leaching test, the same amount of oxygen was supplied  
234 to the samples: 20.6% of oxygen was measured with oxygen meter at the top and the  
235 bottom of the column at the end of drying process. In sample B and D in which the  
236 content of pyrite was high, acidic water, therefore, occurred at the rate comparable to  
237 the amount of oxygen supply, resulting in similar pH at each step of leaching.  
238 Meanwhile, sample A and C showed a gradual increase in pH since only residual sulfide  
239 caused acidic water by reacting with the oxygen supply at each step of leaching. The  
240 decrease of the amount of sulfide in sample A and C with the step of leaching resulted  
241 in the gradual increase in pH. Thus, it was found that the change of pH was dependent  
242 on the sulfur content in rocks and the amount of oxygen supply. There was, moreover, a  
243 sharp drop in pH after 14 days of the drying process in all samples, especially in sample  
244 A, B, and D, as indicated by means of arrows in Figure 3. This suggested that the  
245 amount of oxygen supply during the drying process played an important role in the  
246 progress of AMD. Consequently, the wetting and drying cycle attributed to the supply  
247 of deionized water and the heat of the artificial light accelerated the deterioration in the  
248 water quality with the dissolution of sulfide in the leaching test. The sulfur content in  
249 rocks and the amount of oxygen supply, especially, played an important role in the  
250 change of pH on the basis of the results in this study.

251

252

253

**Fig. 3.**

254

255

### 256 **3.2. Physical Weathering of Rocks**

257 The change of slaking index (SI) of the samples is displayed in Figure 4. The particle  
258 size distribution after the leaching test is described in Figure 5. There was a rapid  
259 increase in SI **at the first step** in sample A, B, and C, followed by a slight increase until  
260 **the fifth step**, whereas SI **gradually increased overall** in sample D in Figure 4. This  
261 result indicated that sample A, B, and C easily **disintegrated** through the wetting and  
262 drying cycle, which is called as a rapid slaking (Tanaka et al., 1997). In contrast, sample  
263 D gradually disintegrated through the wetting and drying cycle. The particle size **of the**  
264 **rock samples** in the columns was set at 1.5-2.0 mm before beginning the leaching test as  
265 shown by a straight line in Figure 5. More than 50% of the rock samples consisted of  
266 less than 0.25 mm of small particles in sample A, B, and C after the leaching test as  
267 indicated by a circle in Figure 5. **The rate of decline of** particle size was consistent with  
268 the change of slaking index in Figure 4, **indicating that** rapid slaking caused a



269 significant decrease of particle size in sample A, B, and C through the wetting and  
270 drying cycle during the leaching test. However, the particle size of approximately 30%  
271 of sample A was more than 1 mm after the leaching test, while that of more than 90% of  
272 sample B, C, and D were less than 1 mm. This was attributed to the prevention of  
273 slaking in sample A due to the compacted layer formed in the surface layer as shown in  
274 Figure 6. Approximately 1 mm of small particles were observed under the compacted  
275 layer at the end of the leaching test in sample A. For these results, the compacted layer  
276 prevented the progress of slaking in sample A, leading to the middle size of the residue  
277 in the column after the leaching test. Although some of the particles in sample A were  
278 not slaked owing to the compacted layer, the decrease of particle size after the leaching  
279 test was observed in all samples.

280 In general, clay minerals cause the disintegration of rocks by slaking with swelling  
281 pressure while swelling and shrinking with the wetting and drying cycle (Karathanasis  
282 et al., 2014). This is considered physical weathering of rocks since the swelling pressure  
283 causes the disintegration of rocks. The clay minerals which have a large specific surface  
284 area compared with other clay minerals, such as kaolinite, montmorillonite, and illite,  
285 significantly contribute to the progress of slaking (Pusch, 1983; Ruiz-Vera and Wu,  
286 2006; Emerson, 1964). In regard to the facts and the result of XRD, kaolinite caused

287 disintegration of rocks by slaking through the wetting and drying cycle in this study.

288 Albite also causes slaking of rocks through the hydrolysis of albite according to the past

289 research, but it is very minor effect (Wen et al., 2014). Other clay minerals causing

290 slaking were not observed in all samples in this study. Therefore, the disintegration of

291 rocks by physical weathering was mainly caused by kaolinite during the leaching test

292 and SI test. In spite of the similar content of kaolinite in all samples, the change of SI of

293 sample D in Figure 4, however, differed from that of the other samples, indicating that

294 the change of SI was affected by other factors in this study. Additionally, the

295 disintegration of rocks can accelerate AMD through the increase of the reactive area of

296 rocks, but the pH remained at low-pH overall in sample B and D with the wetting and

297 drying cycle in Figure 3 even if the rock samples disintegrated due to physical

298 weathering during the leaching test. This also suggested that the change of pH depended

299 on the sulfur content and the amount of oxygen supply more than the effect of physical

300 weathering of rocks.

301

302

303

**Fig. 4.**

304

305

306

307

**Fig. 5.**

308

309

310

**Fig. 6.**

311

312

### 313 **3.3. Chemical Weathering of Rocks**

314 The proportion of the extracted sulfur and iron in the acid extraction test is described

315 by each step of the extraction in Figure 7. The solubility of the elements depends on the

316 existing form of minerals in rocks: sulfate, generally, dissolve in leachate more easily

317 than sulfide (Turkdogan et al., 1974). Thereby, the minerals extracted with HCl affect

318 the water quality in a short time for the high solubility compared with that with HNO<sub>3</sub>,

319 whereas the minerals extracted with HNO<sub>3</sub> contribute to the water quality for a long

320 time owing to the low solubility. In Figure 7, iron and sulfur existed in different form of

321 minerals in the rock samples according to the results: minerals extracted at HCl step, at

322 HF step, and at HNO<sub>3</sub> step. Considering that sulfate can be extracted with HCl and

323 sulfide can be extracted with  $\text{HNO}_3$  in the acid extraction test, more than 81% of sulfur  
324 and iron existed as sulfide in sample D, and approximately 35% of iron and 60% of  
325 sulfur were extracted as sulfide in sample B. Since the high content of sulfide in sample  
326 B and D caused acidic water for a long term, the pH remained at low-pH overall in  
327 sample B and D in Figure 3. Approximately 0-12% of iron and 42-50% of sulfur were  
328 extracted as sulfide, and the sulfur content was 0.83% and 0.03% in sample A and C,  
329 respectively. The ratio of sulfate was, moreover, higher in sample A and C than that in  
330 sample B and D. Hence, most of the soluble sulfates dissolved in the leachate at the  
331 early stage of leaching in sample A and C, leading to a gradual increase of pH in Figure  
332 3. It can, furthermore, be seen that high content of siderite resulted in the highest ratio  
333 of iron extracted with HCl in sample A. In short, the existence form of sulfur and iron in  
334 rocks played an important role in the change of the water quality: this result was  
335 consistent with that of the previous study (Matsumoto et al., 2015).

336 Figure 8 shows the comparison between the amount of extracted iron and sulfur with  
337 HCl and  $\text{HNO}_3$  before and after the wetting and drying cycle. While the amount of  
338 extracted iron and sulfur with  $\text{HNO}_3$  was higher before the wetting and drying cycle,  
339 that with HCl was higher after the wetting and drying cycle in the figure. In terms of the  
340 formation of precipitation and/or sulfate with the occurrence of AMD, they were formed

341 from sulfide during the wetting and drying cycle and dissolved by HCl. Thus, soluble

342 minerals are formed with the occurrence of AMD during the wetting and drying cycle.

343 The amount of sulfur and iron extracted with HCl after the wetting and drying cycle

344 is compared with the amount of dissolved sulfur and iron in the leachate in the simple

345 dissolution test in Figure 9. It suggested that soluble sulfate extracted with HCl was

346 easily dissolved in leachate when they were exposed to water. The amount of dissolved

347 elements was not in good agreement with the amount of extracted iron and sulfur with

348 HCl in sample A and C; however, similar values were obtained in sample B and D.

349 Considering the small amount of sulfur and iron content in sample A and C in Figure 2,

350 the difference was attributed to the heterogeneous distribution of sulfur and iron in

351 rocks. Consequently, the elements which were extracted with HCl easily dissolved in

352 the leachate, leading to AMD in a short time.

353

354

355 **Fig. 7.**

356

357

358

359

360

361

**Fig. 8.**

362

363

364

**Fig. 9.**

365

366

367 Figure 10 shows the surface conditions of the rock samples after the wetting and  
368 drying cycle and the **simple** dissolution test. While the products which are thought of as  
369 oxidative products and/or precipitations were observed on the surface of the samples  
370 after the wetting and drying cycle in Figures 10a<sub>1</sub>, b<sub>1</sub>, c<sub>1</sub>, and d<sub>1</sub>, they were not observed  
371 after the **simple** dissolution test in Figures 10a<sub>2</sub>, b<sub>2</sub>, c<sub>2</sub>, and d<sub>2</sub>. The changes were clearly  
372 observed in sample B and D which contained a large amount of iron and sulfur  
373 compared to that in sample A and C. In addition, micro-cracks were observed on the  
374 surface of the rock samples after the **simple** dissolution test as presented by white  
375 circles in Figure 10a<sub>3</sub>, b<sub>3</sub>, c<sub>3</sub>, and d<sub>3</sub>. Considering that the elements extracted with HCl  
376 dissolved in the **simple** dissolution test, the micro-cracks were developed at the voids

377 which were formed after the dissolution of soluble minerals. According to the previous  
378 research, the dissolution of soluble minerals can lead to the decrease of the strength of  
379 rocks (Tran et al., 2011; Ciantia et al., 2015). The strength decreased and the  
380 micro-cracks occurred as the result of the formation of void after the dissolution of  
381 soluble minerals. This phenomenon was considered chemical weathering of rocks in  
382 this study since the dissolution of soluble sulfur and iron led to the development of  
383 micro-cracks on the surface of rocks. Therefore, chemical weathering of rocks and the  
384 occurrence of AMD progressed simultaneously through the wetting and drying cycle  
385 with the acidification of rocks. Although the chemical weathering caused by dissolution  
386 of soluble iron and sulfur occurred in the leaching test, it can be said that the change of  
387 pH was mainly affected by sulfur content, the existence form of sulfur and iron in rocks,  
388 and the amount of oxygen supply more than the effect of the chemical weathering in  
389 this study.

390

391

392

**Fig. 10.**

393

394

### 395 3.4. Interaction of Physical Weathering and Chemical Weathering of Rocks

396 On the basis of the results as shown above, chemical and physical weathering of  
397 rocks progressed simultaneously with the occurrence of AMD during the wetting and  
398 drying cycle in the argillaceous rocks which contained sulfide and clay minerals related  
399 to slaking. In view of the fact that the physical weathering of rocks causes cracks by  
400 swelling of clay minerals and the chemical weathering causes micro-cracks with the  
401 dissolution of soluble sulfur and iron, physical weathering can be accelerated by  
402 chemical weathering with the development of cracks from micro-cracks as shown in  
403 Figure 11. Physical weathering of rocks by slaking due to swelling of kaolinite and the  
404 hydrolysis of albite and chemical weathering with micro-cracks on the surface of rocks  
405 caused by the dissolution of soluble sulfur and iron occurred with the progress of AMD  
406 during the leaching test and SI test in this study. Given that the proportion of soluble  
407 iron and sulfur in sample A, B, and C was higher than that in sample D by  
408 approximately 30% in the ratio, the occurrence of the micro-cracks on the surface of  
409 rocks with the dissolution of soluble sulfur and iron significantly accelerated the  
410 disintegration of rocks caused by slaking of kaolinite, resulting in the rapid increase of  
411 SI in sample A, B, and C in SI test in spite of the similar amount of kaolinite in all  
412 samples. It was, however, found that the sulfur content, the existence form of sulfur and



413 iron in rocks, and the amount of oxygen supply significantly affected the change of the  
414 water quality although the physical and chemical weathering of rocks could affect the  
415 progress of AMD with the increase of specific surface area through disintegration of  
416 rocks.

417

418

419 **Fig. 11.**

420

421

#### 422 **4. CONCLUSIONS**

423 The interaction between physical and chemical weathering of rocks as well as the  
424 effect of the interaction on AMD were investigated by performing the leaching test,  
425 slaking index (SI) test, and acid extraction test with sample analysis before and after the  
426 wetting and drying cycle. The conclusions are summarized as follows:

427 I. The argillaceous rock which contained sulfide caused chemical weathering  
428 with micro-cracks on the surface of rocks through the dissolution of soluble  
429 iron and sulfur along with the occurrence of AMD.

430 II. The chemical and physical weathering of rocks by swelling of clay minerals  
431 progressed simultaneously with the wetting and drying cycle. Furthermore,  
432 chemical weathering accelerated physical weathering of rocks with the  
433 occurrence of micro-cracks on the surface of rocks after the dissolution of  
434 soluble sulfur and iron.

435 III. Although the disintegration of rocks by physical and chemical weathering  
436 could affect the progress of AMD, the change of the water quality by AMD  
437 over time was significantly affected by the amount of oxygen supply, the  
438 sulfur content, and the existence form of sulfur and iron in rocks more than  
439 the effect of rock weathering.

440

441 **ACKNOWLEDGEMENTS:** The authors would like to express their gratitude and  
442 appreciation to the mine for providing the rock samples in this study. We are also  
443 grateful to engineers in the mine and colleagues in Kyushu University for supporting the  
444 part of the sampling and the analysis.

445

446

447

448    **REFERENCES**

- 449    AMIRA International, 2002, ARD test handbook: prediction & kinetic control of acid  
450       mine drainage, AMIRA P387A. Reported by Ian Wark Research Institute and  
451       Environmental Geochemistry International Ltd. Melbourne, Australia, AMIRA  
452       International.
- 453    Ciantia, O.M., Castellanza, R., Crosta, B.G., and Hueckel, T., 2015, Effects of mineral  
454       suspension and dissolution on strength and compressibility of soft carbonate rocks.  
455       Engineering Geology, 184, 1–18.
- 456    Dold, B., Toril, G.E., Aguilera, A., Pamo, L.E., Cisternas, E.M., Bucchi, F., and Amils,  
457       R., 2013, Acid rock drainage and rock weathering in Antarctica: important sources  
458       for iron cycling in the southern ocean. Environmental Science and Technology, 47,  
459       6129–6136.
- 460    Emerson, W.W., 1964, The slaking of soil crumbs as influenced by clay mineral  
461       composition. Australian Journal of Soil Research, 2, 211–217.
- 462    Huerta-Diaz, A.M. and Morse, W.J., 1990, Quantitative method for determination of  
463       trace metal concentration in sedimentary pyrite. Marine Chemistry, 29, 119–144.

464 Jennings, S.R., Neuman, D.R., and Blicker, P.S., 2008, Acid Mine Drainage and Effects  
465 on Fish Health and Ecology: a Review. Reclamation Research Group Publication,  
466 Bozeman, 26 p.

467 Karathanasis, D.A., Murdock, W.L., Matocha, J.C., Grove, J., and Thompson, L.Y.,  
468 2014, Fragipan horizon fragmentation in slaking experiments with amendment  
469 materials and ryegrass root tissue extracts. The Scientific World Journal, 2014, 1–  
470 13.

471 Lobb, D. and Femmer, S., 2007, Missouri streams fact sheet: watersheds. In: Wolken, S.  
472 (ed.), Missouri Stream Team. Missouri Conservation Department, Jefferson, 1–13.

473 Matsumoto, S., Ishimatsu, H., Shimada, H., Sasaoka, T., Matsui, K., Kusuma, J.G.,  
474 2015, Prevention of acid mine drainage (AMD) by using sulfur-bearing rocks for a  
475 cover layer in a dry cover system in view of the form of sulfur. Journal of the  
476 Polish Mineral Engineering Society, 36, 29-35.

477 Moon, V. and Jayawardane, J., 2004, Geomechanical and geochemical changes during  
478 early stages of weathering of Karamu basalt, New Zealand. Engineering Geology,  
479 74, 57–72.

480 Okawara, M., Yoneda, T., Mitachi, T., and Tada, M., 1996, Mineralogical/chemical  
481 evaluation of shear zone clay for paleo–slip surface determination – A case study

482        inthe Myoukurasawa paleo–landslidearea, Iwate prefecture -. Journal of the Japan  
483        Society of Engineering Geology, 37, 2-13.

484    Pusch, R., 1983, Use of clays as buffers in radioactive repositories. Technical Report  
485        83–46, University of Lulea, Division of Soil Mechanics, Lulea, 86 p.

486    Ruiz-Vera, M.V., and Wu, L., 2006, Influence of sodicity, clay mineralogy, prewetting  
487        rate, and their interaction on aggregate stability. Soil Science Society of America  
488        Journal, 70, 1825–1833.

489    Sadisun, A.I., Shimada, H., Ichinose, M., and Matsui, K., 2003, Further developments  
490        in procedures to determine durability characteristics of argillaceous rocks using a  
491        static slaking index test. Proceedings of the 1<sup>st</sup> International Workshop on Earth  
492        Science and Technology, Fukuoka, November 7, p. 179–186.

493    Sasaki, K., Haga, T., Hirajima, T., and Kurosawa, K., 2002, Distribution and transition  
494        of heavy metals in mine tailing dumps. Materials Transactions, 43, 2778–2783.

495    Wen, B., Li, H., Ke, K., 2014, Effect of soaking on shear strength of weathered  
496        argillaceous rocks susceptible to landsliding in the three gorges area of china. In:  
497        Sassa, K. et al. (ed.), Landslide Science for a Safer Geoenvironment, Vol. 2.  
498        Springer International Publishing Switzerland 2014, 135-140.

499 Tanaka, U., Yokoi, Y., Kosaki, T., and Kyuma, K., 1997, Mechanisms and processes of  
500 crust formation on artificial aggregates: effect of slaking and impact of rain drops  
501 on crusting under different moisture conditions. *Soil Science and Plant Nutrition*, 43,  
502 109–115.

503 Tran, K.M., Shin, H., Byun, Y., and Lee, J., 2011, Mineral dissolution effects on  
504 mechanical strength. *Engineering Geology*, 125, 26–34.

505 Turkdogan, T.E., Rice, B.B., Vinters, V.J., 1974, Sulfide and sulfate solid solubility in  
506 lime, magnesia, and calcined dolomite: part I. CaS and CaSO<sub>4</sub> solubility in CaO.  
507 *Metallurgical Transactions*, 5, 1527-1535.

508

## 509 **Figure Captions**

510

511 **Table 1.** Summary of experiment and the purpose in this study.

512 **Table 2.** Quartz Index (QI) calculated based on the intensity in the result of XRD,

513 **Fig. 1.** X-ray diffraction (XRD) patterns of sample A, B, C, and D. Qz, Ka, Al, Si, and  
514 Py represent quartz, kaolinite, albite, siderite, and pyrite, respectively.

515 **Fig. 2.** Chemical composition of sample A, B, C, and D.

516 **Fig. 3.** Change of pH in sample A, B, C, and D in the leaching test.

517 **Fig. 4.** Change of slaking index (SI) in sample A, B, C, and D.

518 **Fig. 5.** Change of particle size distribution before and after the leaching test: initial size  
519 of the samples was set at 1.5-2.0 mm.

520 **Fig. 6.** Physical conditions of sample A after the leaching test. (a) Physical conditions of  
521 the surface layer in the column from side view. (b) Middle-size particles under the  
522 compacted layer after the leaching test from top view.

523 **Fig. 7.** Proportion of extracted iron and sulfur at each step of the acid extraction. (a)  
524 Proportion of extracted iron. (b) Proportion of extracted sulfur.

525 **Fig. 8.** Comparison of the amount of extracted iron and sulfur with HCl and HNO<sub>3</sub>  
526 before and after the wetting and drying cycle. (a) Comparison of the amount of  
527 extracted iron. (b) Comparison of the amount of extracted sulfur.

528 **Fig. 9.** Comparison of the amount of extracted iron and sulfur with HCl in the acid  
529 extraction test and that of dissolved iron and sulfur in the simple dissolution test. (a)  
530 Comparison of the amount of soluble iron. (b) Comparison of the amount of soluble  
531 sulfur.

532 **Fig. 10.** Surface conditions of sample A, B, C, and D. Symbol of “a, b, c, d” represents  
533 sample A, B, C, and D, respectively. (1) After the wetting and drying cycle. (2) After

534 the simple dissolution test. (3) Micro-crack on the surface of rocks after the simple  
535 dissolution test.

536 **Fig. 11.** Interaction between physical and chemical weathering of rocks.